The ion trap aerosol mass spectrometer: improved design, first field deployment, and the capability of differentiating organic compound classes via MS-MS

Johannes R. W. Fachinger[1], Stéphane J. Gallavardin[1,2], Frank Helleis[3], Friederike Fachinger[1], Frank Drewnick[1], Stephan Borrmann[1,2]

[1]Particle Chemistry Department, Max Planck Institute for Chemistry, Mainz, 55128, Germany
[2]Institute for Atmospheric Physics, Johannes Gutenberg University Mainz, Mainz, 55128, Germany
[3]Max Planck Institute for Chemistry, Mainz, 55128, Germany

Correspondence to: Stephan Borrmann (stephan.borrmann@mpic.de)

Abstract. Further development and optimisation of a previously described ion trap aerosol mass spectrometer (IT-AMS) are presented, which resulted in more reproducible and robust operation and allowed for the instrument's first field deployment. Results from this 11-day long measurement indicate that the instrument is capable of providing quantitative information on organics, nitrate, and sulphate mass concentrations with reasonable detection limits ($0.5 - 1.4$ μg m^{-3} for 1 h averages), and that results obtained with the IT-AMS can directly be related to those from Aerodyne aerosol mass spectrometers. The capability of the IT-AMS to elucidate the structure of fragment ions is demonstrated via an MS^4 study on tryptophan. Detection limits are demonstrated to be sufficiently low to allow for MS^2 studies not only in laboratory, but also in field measurements under favourable conditions or with the use of an aerosol concentrator. In laboratory studies the capability of the IT-AMS to differentiate $[C_4H_y]^+$ and $[C_3H_yO]^+$ fragments at the nominal *m/z* 55 and 57 via their characteristic fragmentation patterns in MS^2 experiments was demonstrated. Furthermore, with the IT-AMS it is possible to distinguish between fragments of the same elemental composition ($[C_2H_4O_2]^+$ at *m/z* 60 and $[C_3H_5O_2]^+$ at *m/z* 73) originating from different compound classes (carboxylic acids and sugars) due to their different molecular structure. These findings constitute a proof of concept and could provide a new means of distinguishing between these two compound classes in ambient organic aerosol.

Keywords: ion trap; aerosol mass spectrometry; sugar; carboxylic acid; structure determination

1 Introduction

Despite the fact that atmospheric aerosol particles have an important influence on air quality, public health, and the climate system, the knowledge on the influence of individual aerosol particle chemical components remains limited (Fuzzi et al., 2015). One main contributor to fine particulate matter is organic aerosol (Kanakidou et al., 2005), which includes a large variety of different, to a large part unknown, organic molecules (Goldstein and Galbally, 2007).

Much work has been invested in the past in order to chemically characterise the organic material present within the ambient aerosol, mostly using mass spectrometric techniques (Hoffmann et al., 2011). For off-line analyses of filter samples from atmospheric aerosol particles, mass spectrometry is often coupled to chromatographic methods for prior separation of the organic compounds (Pratt and Prather, 2012), while with the most commonly used on-line techniques either single particles

5 (Murphy, 2007; Silva and Prather, 2000) or small ensembles of particles (Canagaratna et al., 2007) are analysed without prior separation of substances.

The currently most widely used instrument deploying the latter method is the Aerodyne aerosol mass spectrometer (AMS, Aerodyne Inc.; Jayne et al., 2000), in which ensembles of particles are flash-vaporised at typically ~600 °C and the evolving vapour is ionised by electron impact ionisation before mass spectrometric analysis, usually with a time of flight mass

10 spectrometer (ToF-AMS; Drewnick et al., 2005; DeCarlo et al., 2006). Since here a large number of different molecules is analysed simultaneously, mathematical algorithms have to be applied to the acquired mass spectra in order to obtain information on different particle components (Allan et al., 2004). Due to the thermal desorption and "hard" electron impact ionisation, molecules are strongly fragmented, which means a partial loss of the original molecular information. On the other hand, this considerably reduces the complexity of information when dealing with mixtures of a large variety of different

15 organic compounds (Hoffmann et al., 2011) while some important information on the original molecular structures are still retained, which enables the determination of "types" of organic particle constituents using positive matrix factorisation (Zhang et al., 2011).

The differentiation of organic components can be further constrained and improved using the high resolution ToF-AMS, which has a mass resolution of ~2000 or ~4000 in two modes providing higher and lower sensitivity, respectively (DeCarlo

20 et al., 2006). With these resolutions, it is possible to distinguish between isobars, i.e., ion fragments of the same nominal mass to charge ratio (m/z), but with different elemental compositions. For example, a prominent mass spectral signal at m/z 55 is observed in both hydrocarbon-like (traffic-related) and cooking-related organic aerosol. While this signal seems to be related mostly to $[C_4H_7]^+$ in hydrocarbon-like organic aerosol, an additional large fraction of $[C_3H_3O]^+$ at the same nominal m/z is found for cooking-related organic aerosol (Sun et al., 2011).

25 While some information on elemental composition of the fragment ions can be obtained with the ToF-AMS, it does not allow for the differentiation between fragment ions of the same elemental composition, but with different structural formulas. Such information can be obtained using ion trap mass spectrometers (March, 1997), which allow not only for measuring a "classic" mass spectrum (MS), but enable also MS^n studies. In such experiments, ions of a single nominal m/z are first isolated and then fragmented by collisions with buffer gas atoms (collision induced dissociation, CID). The resulting

30 fragment ions can be either mass scanned, which provides the mass spectrum of the fragment ions (MS-MS, or MS^2), or again ions of a certain m/z can be separated and fragmented, and so on (MS^n). From the fragment ions and fragmentation pathways, conclusions on the molecular structure of the parent ion can be drawn (March, 1997; McLafferty and Tureček, 1993).

Due to their capability to elucidate the molecular structure of organic molecules, ion traps are often coupled to "soft" ionisation techniques, in order to preserve the molecular structure of the compounds of interest as much as possible. For atmospheric applications, e.g., vacuum ultraviolet single photon ionisation (Hanna et al., 2009), proton transfer reaction (Thornberry et al., 2009), and atmospheric pressure chemical ionisation (Vogel et al., 2013) have been successfully applied

5   in conjunction with ion trap mass spectrometry. Kürten et al. (2007) introduced an instrument which represents a synthesis of an AMS ionisation chamber (thermal desorption / electron impact ionisation) with a quadrupole ion trap mass spectrometer; a similar instrument was also developed by Harris et al. (2007). With these systems, a strong reduction in complexity of organic aerosol mass spectra is achieved compared to "soft" ionisation techniques, while still some additional information, e.g., on molecular functionality can be obtained which is not accessible from ToF-AMS measurements.

10   Here, we present further design improvements of the ion trap aerosol mass spectrometer (IT-AMS) originally introduced by Kürten et al. (2007). Technical improvements enable more robust and reproducible measurements with this instrument since the work of Kürten et al. (2007) and allowed for the instrument's first field deployment. We show how the IT-AMS compares with a regular ToF-AMS and demonstrate its MS^n capability up to MS^4, also providing an estimate of the related detection limits. Finally, from MS^2 studies on various compounds, we demonstrate how the IT-AMS is capable of

15   distinguishing between fragment ions of different molecular structures even if they have the same elemental composition, which could provide a means to distinguish between – and potentially quantify – carboxylic acids and sugars in organic aerosol.

2 Instrumental developments

The original setup and the working principle of the ion trap aerosol mass spectrometer (IT-AMS) are described in detail in

20   (Kürten et al., 2007). Here, only a brief overview of the instrument is given (Fig. 1). The instrument consists of the same commercially available particle inlet and ionisation chamber as contained in the AMS (Jayne et al., 2000), coupled to a home-built quadrupole ion trap (Kürten et al., 2007). Sub-micron sized particles entering the instrument are focused by a Liu-type aerodynamic lens (Liu et al. (1995); see (Fachinger, 2012) for details on the lens characteristics). A shutter located behind the inlet can be either closed to block the particle beam (measurement of instrumental background) or opened

25   (particle beam plus background), enabling the calculation of "difference" mass spectra (open minus closed) originating purely from the particle beam (Canagaratna et al., 2007). In the ionisation chamber the particles are flash-vaporised on a hot tungsten surface (~600 °C), and the resulting vapour is ionised by electron impact ionisation (70 eV). The ions are extracted through ion optics to the quadrupole ion trap, which consists of a ring electrode and two hyperbolical end cap electrodes with modified angle geometry with $r_0 = 1$ cm and $z_0 = r_0/\sqrt{1.9} = 0.725$ cm, where r_0 and z_0 are the shortest distances from the

30   centre of the trap to the ring and end cap electrodes, respectively. In the ion trap, the ions can be stored and manipulated; ions leaving the trap are then detected using a channeltron (KBL510, Sjuts). High purity helium is used as buffer gas in the ion trap.

While the instrument described in (Kürten et al., 2007) was capable of providing quantitative information on aerosol components, it suffered from a lack of user-friendliness and from limited long-term stability and reproducibility of the measurements. Therefore, in order to prepare the instrument for field measurements and regular laboratory applications, several hardware (electronical and mechanical) as well as instrument control software modifications were performed, all

5   aiming at a more robust, versatile, and user-friendly operation of the instrument. The operation principles for the MS and MS^n measurements, e.g., mass range extension, ion isolation, and ion excitation and fragmentation, were nevertheless kept the same. We only describe the most important changes in detail here; other modifications are only briefly summarised and their details can be found in (Fachinger, 2012).

Most importantly, three hardware modifications related to the mechanical design of the instrument were realised (see Fig. 1,

10   inserts):

- In the ion trap, instead of the ceramic washers used by Kürten et al. (2007) as spacers between the ring and end cap electrode, now ruby spheres (diameter 6 mm ± 0.635 µm) sitting in precise countersinks (1.3 mm ± 10 µm) are used for a more defined mounting (insert B). This allows for a more reproducible assembly of the electrodes, and consequently more reproducible voltage settings.

15   - In order to ensure stable and reproducible ion signal intensities, constant helium pressure in the ion trap is needed, which is achieved in the IT-AMS by a constant inlet mass flow of helium and constant pumping speed. In the original setup, this helium inlet flow was regulated via a needle valve, and therefore changed with changing ambient (upstream) pressure. Now, constant inlet mass flow is provided by a critical orifice with constant upstream pressure ensured by a pressure-controlled mass flow controller (insert A). With this system, the pressure inside the system

20   ($7 \cdot 10^{-5}$ hPa, measured outside the trap) was found to be stable within 1 % (relative standard deviation of 15 s data) over the course of eleven days.

- The ion trap needs a pulsed ion source so that ions are only generated and transmitted to the ion trap during the trapping phase, but not during the analysis phase. This was realised in the original setup by gating of the ion source cage voltages (Kürten et al., 2007): only during the trapping phase, electrons were accelerated into the ion source

25   cage, while in the other phases, they were deflected from it. This led to an instable filament emission current directly after switching the voltages, potentially due to the build-up of space charges. Now, a more stable filament emission current (and therefore better reproducibility) is achieved by the use of a modified filament which allows for pulsed ion source operation: electrons emitted by the filament are now either deflected or absorbed by a deflection plate (insert C), depending on whether they are needed in the ion source or not.

30   Also on the electronic parts of the instrument, several smaller modifications (the capacitive coupling between the ring / end cap electrodes of the ion trap, the radiofrequency voltage generator, and the housing was improved; more flexible and robust electrical and communication connections of the electronics controller with the instrument; and integration of a vacuum interlock) were performed aiming at enhanced stability and reproducibility, easier handling, and improved flexibility. These modifications are described in detail in (Fachinger, 2012).

The IT-AMS is controlled via a program written in LabVIEW (National Instruments), which is also utilised for data acquisition. As detailed in (Fachinger, 2012), this software was extended and now allows for semi-automatic tuning of operation parameters, flexibility in the measurement types and their operating conditions (MS, MS^2, $MS^{n>2}$ ($n \leq 5$), mass range extension), programming long series of measurements, and the control of the shutter to enable automatic switching between open / closed measurements, as described above. Furthermore, all instrumental settings and parameters are now saved along with the mass spectra after each measurement cycle.

3 Laboratory and field measurements

In the laboratory studies, particles were typically generated from an aqueous solution of the respective substance (Table 1) using a nebuliser (model 3076, TSI Inc.). Oleic acid was dissolved in ethanol instead of water (in case of the ToF-AMS, an aqueous suspension was used), while butyl valerate in both cases was leaked as vapour directly into the instrument. After generation, the aerosol was dried using two consecutive silica gel diffusion driers before sampling with the IT-AMS or high resolution ToF-AMS (DeCarlo et al., 2006), respectively. For the determination of the MS^n detection limits using tryptophan (Sect. 4.2), monodisperse aerosol (130 nm mobility diameter) was generated by classifying the dried particles using a differential mobility analyser (model 3081, TSI Inc.). Parallel measurement of particle number concentration using a condensation particle counter (model 3025A, TSI Inc.) enabled the calculation of the sampled aerosol mass concentration, assuming spherical particles with the bulk density of tryptophan (1.34 g cm^{-3}).

Continuous measurements of ambient aerosol using the IT-AMS and a high resolution ToF-AMS were concurrently performed on the Mt. Kleiner Feldberg (Central Germany) from 29 August to 09 September 2011 (Sobanski et al., 2016). Both instruments were sampling in parallel through two separate inlets (7 m a.g.l), which were located in about 5 m distance from each other. The IT-AMS was measuring with a time resolution of 30 s (10 s particle beam blocked, 10 s open, with 5 s waiting time between each half-cycle; during each 10 s interval 100 mass spectra were averaged, each acquired after 50 ms ion accumulation time), the ToF-AMS with a resolution of 60 s (containing 15 s beam blocked, 15 s open, and 30 s size distribution measurement).

In all laboratory and field measurements, ions were trapped over 50 ms at a radiofrequency (1.3 MHz) drive voltage of 250 to 700 V amplitude (zero-to-peak) applied to the ion trap ring electrode. To reach the maximum m/z of 135 used within this work, in the laboratory experiments – if needed – the mass range was extended by applying an additional voltage of 400 mV amplitude (zero-to-peak) with a frequency of 400 kHz to both end cap electrodes. In MS^n experiments, ions of m/z of interest were isolated (typically within a range of $\pm$ 5 m/z) by broad band excitation using a filtered noise field (Julian and Cooks, 1993) before they were fragmented using collision induced dissociation (CID, see parameters in Table 2).

Measured IT-AMS mass spectral signals were converted to ion rates (during the trapping phase) and integrated to unit mass resolution (UMR) mass spectra using home-built procedures in IGOR Pro (WaveMetrics Inc.) and MATLAB (MathWorks). High resolution ToF-AMS data were analysed using SQUIRREL v.1.44 and PIKA v.1.04 and higher (SQUIRREL, 2016).

From the ToF-AMS field data, organics, nitrate, and sulphate mass concentrations were determined using the fragmentation pattern table (Allan et al., 2004) within SQUIRREL (v.1.51H), corrected for background effects using routinely performed measurements of particle-free air. Ionisation efficiency of the ToF-AMS was determined prior to the campaign. A collection efficiency of 50 % was applied following Canagaratna et al. (2007), which resulted in good agreement with other co-located measurements (Fachinger, 2012).

For the IT-AMS field data, difference mass spectra were calculated from the UMR mass spectra obtained during beam open and blocked time. From these, species-resolved total ion rates for organics, nitrate, and sulphate were calculated using a simplified fragmentation pattern table (due to reduced signal to noise ratio) by summing the mass spectral signal of the m/z containing the respective species' dominant ions in the m/z range $30 - 106$ (nitrate: m/z 30, 46; sulphate: m/z 48, 64, 80, 81, 98; organics: all other m/z except 32, 39, 40).

4 Results and discussion

4.1 Measurement of ambient aerosol: comparability to ToF-AMS results

Figure 2 shows a comparison of the average mass spectra from the IT-AMS and the ToF-AMS, acquired during 11 days of field measurement. The m/z 30 and above are colour-coded for the species (organics, nitrate, sulphate) which they are dominantly associated with (see Sect. 3). Here, we discuss general trends on the basis of the campaign average in order to minimise the statistical uncertainty. The same features are typically also visible when comparing 1 h averaged mass spectra; in that case the observed trends are more distinct at higher absolute mass concentration (i.e., at higher signal to noise ratio).

Strong differences between the mass spectra are observed in the m/z range below 30. This is probably mostly due to the strong influence of charge-transfer reactions in the ion trap during the trapping phase in this m/z range, e.g., involving N^+, O^+, N_2^+, or O_2^+ (Dotan et al., 1997; Hierl et al., 1997). m/z 28 (N_2^+), 32 (O_2^+) and 40 (Ar^+), but also m/z 44 (CO_2^+) are depleted in the IT-AMS compared to the ToF-AMS mass spectrum, likely due to formation of more stable ions by charge-transfer reactions in the ion trap (Ottens et al., 2005). Furthermore, the ratio of m/z 18 to m/z 19 (H_2O^+ to H_3O^+) is much smaller in the IT-AMS mass spectrum compared to that of the ToF-AMS, probably caused by proton transfer reactions occurring in the ion trap ($H_2O + H_2O^+ \rightarrow H_3O^+ + \cdot OH$, (Cole et al., 2003)). In laboratory experiments, we found that with increasing ion accumulation and reaction times, this ratio decreases exponentially, converging to a ratio of ~1:1 at accumulation times $\geq$200 ms. Beside these differences, a plateau of more or less constant relative signal intensity is observed from m/z 20 to 27 for the IT-AMS (Figure 2, lower panel), but not for the ToF-AMS. Kürten (2007) found that this plateau disappears when an additional reaction time is applied to allow for collisional cooling (Wu and Brodbelt, 1992). It can therefore be considered an artefact. In this work, we focus on m/z 30 and above, since the deconvolution of ion signal below m/z 30 is complicated due to the contribution of several species to most single m/z (Allan et al., 2004) and the relatively strong influence of artefacts in this m/z range.

Considering the organics signal at m/z >30, most strikingly, an increasing signal ratio (IT-AMS / ToF-AMS) with increasing m/z is observed (Figure 2, upper panel). This probably is explained by different ion transmission efficiency curves with respect to m/z for the two instruments, which can easily be accounted for by calibrations. Importantly, though, the fragmentation pattern (Figure 2, lower panel) is comparable between both instruments, despite the much longer residence

5   time of the ions in the ion trap (50 ms accumulation time) compared to the ToF-AMS. Thus results obtained with the IT-AMS, including MS-MS measurements, are directly transferable to ToF-AMS measurements. This comparability needs to be validated also for other accumulation and reaction times.

In contrast, signals of m/z mostly related to sulphate fragments are strongly depleted in the IT-AMS compared to the ToF-AMS mass spectrum, and also the fragmentation pattern is different. The signal ratio of m/z 48 to 64, which are dominated

10   by the sulphate ion fragments SO^+ and SO_2^+, is 0.8 in the ToF-AMS mass spectrum, but 1.7 in that of the IT-AMS, despite the opposing trend of ion transmission efficiency. Both decomposition of the ions and charge-transfer reactions (with different efficiency for different ions) could cause this ion depletion and fragmentation pattern changes. This needs to be further investigated, also as a function of accumulation and reaction times. Contrary, for nitrate-related ions, no depletion in the IT-AMS has been found.

15   Figure 3 shows the measured organics, nitrate, and sulphate concentration time series for both instruments. No calibration measurements were performed for the IT-AMS, whose results are therefore reported in ion rates. For all three species, the time series measured with IT-AMS and ToF-AMS correlate linearly over the range of observed mass concentrations (Fig. 3), confirming the capability of the IT-AMS to quantitatively measure species mass concentrations using adequate calibrations for all species, as demonstrated for nitrate by Kürten et al. (2007). The squared Pearson's correlation coefficients for 10 min

20   (1 h) averaged time series are 0.82 (0.88) for organics, 0.68 (0.65) for nitrate, and 0.37 (0.58) for sulphate (Fig. 3). The much lower correlation coefficient for sulphate compared to the other species is in agreement with the observation of much lower response (and therefore, lower ion rates and signal-to-noise ratio) of the IT-AMS for sulphate than for nitrate and organics (Figs. 2 and 3).

Detection limits for organics, nitrate, and sulphate are calculated following the method by Drewnick et al. (2009). For this,

25   ion rates measured with the IT-AMS are converted to mass concentrations using the linear relationship with the ToF-AMS results (Fig. 3). Detection limits for 10 min (1 h) averages are 3.7 µg m^{-3} (1.4 µg m^{-3}) for organics, 1.3 µg m^{-3} (0.5 µg m^{-3}) for nitrate, and 1.3 µg m^{-3} (0.7 µg m^{-3}) for sulphate. The higher detection limit for organics can be explained by the fact that the mass spectral signal is distributed over a much larger number of m/z (Fig. 2), thereby lowering the signal-to-noise ratio. For all three species, the detection limits found for the IT-AMS are two to three orders of magnitude higher than those

30   reported for the ToF-AMS (DeCarlo et al., 2006; Drewnick et al., 2009), due to much lower ion rates (by three orders of magnitude). Thus, the IT-AMS is capable of providing absolute mass concentrations of organics, nitrate, and sulphate at typical ambient concentrations, e.g., in urban areas (i.e., in the order of several µg m^{-3}) after application of adequate calibrations.

4.2 Prospects and limitations of MS[n] studies

While the IT-AMS has lower sensitivity compared to the ToF-AMS, it allows for more detailed, in-depth studies of the measured aerosol. Using MS[n] studies, it is possible to derive structural information on the measured ions, while with the ToF-AMS, only information on their elemental composition can be obtained.

5   In this section, we discuss the potential of MS[n] studies with the IT-AMS exemplarily by means of results obtained for two compounds: glutathione and tryptophan (Table 1). Their "classic" mass spectra, obtained with the IT-AMS, are shown in Figs. 4a (glutathione) and 5a (tryptophan). Both show prominent ion signals at m/z 130, which judging from the structure of the respective parent molecules are likely from $[C_5H_8O_3N]^+$ (glutathione) and $[C_9H_8N]^+$ (tryptophan). With the ToF-AMS, these would be possible to distinguish only in the mode of highest mass resolution (~4000), but not in the more sensitive

10   mode of lower mass resolution (~2000) (DeCarlo et al., 2006). With the IT-AMS, they can be distinguished by means of MS-MS (MS[2]): CID of m/z 130 yields the fragment ions m/z 103 ($[C_8H_7]^+$) and m/z 128 ($[C_9H_6N]^+$) for tryptophan (Fig. 5b), but m/z 83 ($[C_4H_5ON]^+$) and m/z 84 ($[C_4H_6ON]^+$) for glutathione (Fig. 4b), revealing the different nature of their respective parent ions.

The resulting ions (from MS[2]) can be further fragmented in order to obtain more detailed information on their molecular

15   structure, as shown for tryptophan in Fig. 5c,d: CID of m/z 103 yields m/z 77 ($[C_6H_5]^+$) (MS[3]); the thereby formed ion at m/z 77 can be further fragmented to m/z 50 ($[C_4H_2]^+$) and m/z 51 ($[C_4H_3]^+$) (MS[4]). When trying to fragment these ions (MS[5]), no ions (neither remaining parent ions at m/z 50 / 51, nor any fragments) could be detected. This could be because the ions are very stable and therefore are removed from the ion trap, even at very low amplitudes for resonant excitation; or because they are fragmented to ions of m/z <20, which were not analysed in the present study.

20   Further information on the nature of the ions observed in the "classic" MS can be obtained by comparing the CID products of different ions from the original mass spectrum (i.e., MS[2] of these ions) with those of the fragmentation chain (MS[3–5]) of larger (parent) fragment ions: While MS[2] of m/z 103, 77, and 50 results in the same fragment ions as observed in the respective MS[3–5] studies of m/z 130 presented above, MS[2] of m/z 51 yields different results. Here, m/z 39 ($[C_3H_3]^+$) and m/z 63 ($[C_5H_3]^+$) are formed while in the fragmentation chain no further fragmentation was observed for this ion. Therefore,

25   it can be concluded that additionally to the fragmentation product of m/z 77 (i.e., $[C_4H_3]^+$), also the doubly charged ion $[C_8H_6]^{2+}$ contributes to m/z 51 in the "classic" MS of tryptophan. The ions $[C_4H_3]^+$ and $[C_8H_6]^{2+}$ would not be possible to distinguish with the ToF-AMS.

The detection limits of the tryptophan MS[n] experiments were calculated following Drewnick et al. (2009) from the standard deviations of the signal intensities at the investigated m/z in a blank MS[n] measurement, and the signal intensity

30   enhancements at the same m/z during MS[n] measurements of known tryptophan mass concentrations. All detection limits were calculated for averages of 3000 mass spectra, which correspond to measurement times of 6, 16, 28, and 46 minutes for the full MS, MS[2], MS[3], and MS[4] cycles, respectively. The corresponding detection limits were found to be ~0.6, 7, 13, and 30 µg m^{-3} at the given measurement conditions. This suggests that MS[2] studies might be feasible under favourable conditions

at ambient concentrations, while $MS^{n>2}$ studies are only possible at high mass concentrations, as, e.g., in smog chamber studies or by applying an aerosol concentrator.

4.3 Differentiation of organic compound classes

In this section, we investigate how the IT-AMS is capable of distinguishing fragments of the same nominal mass, but with

5   different molecular and/or structural formulas. This makes it not only possible to distinguish, e.g., between hydrocarbon-like and oxygenated organic species (Zhang et al., 2011), but potentially also between species with different functional groups, which would allow for the assignment of measured organic species to different compound classes. This potential is investigated by means of MS^2 studies on various substances from different compound classes, particularly sugars and carboxylic acids (Table 1).

10   **4.3.1 Differentiation of ions of the same nominal mass, but with different molecular formulas**

The differentiation of ions of the same nominal m/z, but with different molecular formulas allows, e.g., for the distinction between hydrocarbon-like and oxygenated organic species. This kind of information is also accessible with a high resolution ToF-AMS, given the resolution at the respective m/z is sufficiently high, and is commonly retrieved from such data (Zhang et al., 2011). Here, we demonstrate how the IT-AMS is also capable of providing such information. Figure 6 shows a

15   compilation of results from MS^2 studies on m/z 55 and 57 for a variety of compounds. Also shown is the relative contribution of the major ions at these m/z measured with a ToF-AMS (left panels): $[C_3H_3O]^+$ and $[C_4H_7]^+$ at m/z 55, and $[C_3H_5O]^+$ and $[C_4H_9]^+$ at m/z 57.

When fragmenting the ions at m/z 55 and 57 in the IT-AMS (MS^2), clear differences in the resulting fragmentation patterns are observed between the different compounds. For sugars (glucose, saccharose, mannitol, levoglucosan; reddish/brownish

20   colours in Fig. 6), but also for succinic and glutaric acid (carboxylic acids, bluish colours in Fig. 6), fragmentation occurs predominantly by loss of CO (28 Da, resulting in m/z 27 and 29 ions from parent ions at m/z 55 and 57, respectively). This points to $[C_3H_yO]^+$ as the dominant parent ion for these compounds. Additionally, loss of CH_2O (30 Da) is observed for MS^2 of m/z 57, yielding the fragment ion m/z 27 ($[C_2H_3]^+$), while for MS^2 of m/z 55 for some of these compounds, loss of C_2H_2 (26 Da) results in the fragment ion m/z 29 ($[COH]^+$). Ion recovery is rather low for these compounds for MS^2 of m/z 55

25   (<20 %), and slightly higher for m/z 57 (~40 %).

In contrast, MS^2 studies on oleic acid and butyl valerate reveal the dominant presence of $[C_4H_y]^+$ fragment ions at the nominal masses m/z 55 and 57, consistent with the structure of the respective molecules (with long hydrocarbon chains, greenish colours in Fig. 6) and with results from corresponding ToF-AMS measurements (Fig. 6, left): For m/z 55, predominantly loss of H_2 (2 Da), CH_4 (16 Da), and C_2H_2 (26 Da) is observed. Less abundant is the fragment ion m/z 27,

30   originating from the loss of C_2H_4 (28 Da). For m/z 57, predominantly fragmentation to m/z 41 (loss of CH_4, 16 Da) is found. Ion recovery for MS^2 on these $[C_4H_y]^+$ fragments was found to be much better (50 – 100 %) than for the $[C_3H_yO]^+$ fragments discussed above.

For pinonic acid and PEG200 (polyethylene glycol; see Table 1), no clear picture is obtained. For both compounds, MS^2 studies suggest dominance of $[C_4H_7]^+$ at m/z 55, with fragmentation patterns similar to those of oleic acid and butyl valerate. While this is comprehensible from the molecular structure for pinonic acid, for which also ToF-AMS results show a strong fraction of $[C_4H_7]^+$ at m/z 55, for PEG200, dominance of $[C_3H_3O]^+$ would have been expected both from the molecular

5 structure and from the ToF-AMS measurement (Fig. 6). This needs to be further investigated; it might be possible that the oligomeric structure of PEG200 plays a role here, which could lead to multiply charged larger ion fragments, and to ion rearrangements, and therefore to a different molecular structure of the ion with the elemental composition $[C_3H_3O]^+$ and a different MS^2 mass spectrum. For m/z 57, on the other hand, both PEG200 and pinonic acid show fragmentation patterns originating from $[C_3H_5O]^+$, and only small contributions at m/z 41 which likely originate from fragmentation of $[C_4H_9]^+$. This

10 is consistent with the absence of straight hydrocarbon chains in the molecular structures of these compounds (Table 1), and with the results from the respective ToF-AMS measurements (Fig. 6, left).

These findings show that it is generally possible to distinguish between compounds containing straight hydrocarbon chains and such that do not contain them by MS^2 experiments on m/z 55 and 57. Our results suggest that combined information from the MS^2 fragmentation patterns and the corresponding ion recoveries could facilitate the quantitative determination of

15 the relative contributions of the different ions ($[C_3H_yO]^+$ vs. $[C_4H_y]^+$) to these parent m/z. More work with a larger number of different compounds and under a larger range of operating conditions (in particular also for different vaporisation/ionisation as well as MS^2 fragmentation conditions) is needed in order to test further this assumption and to develop a robust method for the quantification of the relative contributions of these ions to nominal m/z 55 and 57.

4.3.2 Differentiation of ions with the same molecular formula, but different molecular structures

20 While differentiation of ions with the same nominal mass, but different molecular formulas is possible both with the IT-AMS and the ToF-AMS, the differentiation of ions of the same elemental composition, but with different molecular structures is unique to instruments such as the IT-AMS. This feature has already been demonstrated in Sect. 4.2 in the differentiation of singly and doubly charged fragments at m/z 51 in the case of tryptophan, and is further investigated here for ions of the nominal m/z 60 and 73 for a number of carboxylic acids and sugars.

25 In Fig. 7, results from ToF-AMS measurements and IT-AMS MS^2 studies on m/z 60 and 73 are summarised for a variety of sugars (reddish/brownish colours) and carboxylic acids (bluish colours). For m/z 73, also measurements of the polyether PEG200 (pink colour) are included in the figure. ToF-AMS measurements indicate the dominant contribution of ions $[C_2H_4O_2]^+$ and $[C_3H_5O_2]^+$ to m/z 60 and 73, respectively, for both sugars and carboxylic acids (Fig. 7, first column). MS^2 measurements with the IT-AMS, however, reveal differences in the molecular structure of these fragments between the two

30 compound classes, which can be utilised for the differentiation between the latter.

While the ion at m/z 60 from sugars in MS^2 experiments fragments only to ions of m/z 42 by loss of water (18 Da), for carboxylic acids additionally a small contribution of the fragment m/z 43 (loss of OH, 17 Da) is observed (Fig. 7a). This can be explained by different molecular structures of the parent ions $[C_2H_4O_2]^+$ for the two compound classes, which can be

deduced from the molecular structures of the respective parent compounds (Table 1): For sugars, the fragment ion $[C_2H_4O_2]^+$ most likely consists of a diol, with two OH groups attached to two carbon atoms adjacent to each other. In contrast, in the fragment ion of the same molecular formula formed from fragmentation of carboxylic acids, both oxygen atoms most likely are attached to the same carbon atom, forming a carboxyl group. Alcohols fragment predominantly by loss of water, while

5   carboxyl groups are known to also fragment by loss of OH (McLafferty and Tureček, 1993), which is in agreement with our findings. For all investigated compounds, ion recovery was found to be 100 %.

Also in MS^2 experiments on m/z 73 ($[C_3H_5O_2]^+$), differences in the fragmentation chains of carboxylic acids and sugars were observed (Fig. 7b). While m/z 73 from sugars predominantly fragments by loss of CO (28 Da) to ions of m/z 45, for m/z 73 from carboxylic acids this fragmentation pathway is less important, and in contrast it is fragmented predominantly by loss of

10 water (18 Da) to ions of m/z 55. Notably, ion recovery was found to be very different for the two compound groups, with ~100 % ion recovery for carboxylic acids, but only ~60 % for sugars, pointing to an additional fragmentation pathway for m/z 73 from sugars which was not traceable under the given measurement settings. Interestingly, the polyether PEG200 shows a similar fragmentation pattern of m/z 73 as sugars, but with ~100 % ion recovery, pointing to yet another molecular structure of the ion with the chemical formula $[C_3H_5O_2]^+$.

15 These results indicate that with the IT-AMS, it should be possible to determine the relative contributions of carboxylic acids and sugars to the ions m/z 60 and 73 (even though they have the same elemental composition), given no major contributions from other compound classes are present. For MS^2 on m/z 60, the ratio of relative intensities of the fragment ions m/z 43 to m/z 42 is a direct indication for the relative contribution of carboxylic acids to the parent ion: the ratio was found to be (0 / 100 %) for the sugars, but in the range (11 ± 1) % / 100 % for the tested carboxylic acids (Fig. 7a). For MS^2 on m/z 73,

20 the ratio of relative intensities of the fragment ions m/z 45 to m/z 55 was on average 100 % / 3 % (range 100 % / (2 − 5) %) for sugars, and 32 % / 100 % (range (13 − 57) %) / 100 %) for carboxylic acids (Fig. 7b).

Using these results and the average relative contributions of m/z 60 and 73 to the mass spectra of sugars and carboxylic acids, in principle the absolute contribution of these compound classes to the measured total organic mass concentration could be determined from MS^2 experiments on ions of m/z 60 and 73, which would not be possible with the regular ToF-

25 AMS. More work is needed in order to test this possibility with a large number of compounds, concentration ranges, range of operating parameters (especially different MS^2 fragmentation conditions and vaporisation/ionisation conditions), and also for mixtures of compounds. In first sensitivity studies for MS^2 on m/z 73, we already found the presented differentiation to be robust for different aerosol loads, ion quantities in the trapping volume, and ion trapping parameters q_z (see March, 1997). Further characterisation and calibration work is needed in order to fully facilitate quantification of the presented compound

30 classes with the IT-AMS with more robust average values, and to identify the associated limitations and uncertainties, like, e.g., the cross-sensitivity observed for the polyether PEG200 at m/z 73.

5 Summary and conclusion

An ion trap aerosol mass spectrometer (IT-AMS) was further developed and optimised, now allowing for more reproducible and reliable measurements while the instrument is also more robust and user-friendly and has extended measurement capabilities implemented in its data acquisition software. This allowed for the instrument's first, 11-day long field deployment, during which it was continuously running in parallel to a regular ToF-AMS. The results show that the IT-AMS is capable of providing quantitative information on the major non-refractory submicron species organics, nitrate, and sulphate, with detection limits between 0.5 and 1.4 µg m^{-3} for 1 h-averages. IT-AMS and ToF-AMS apply the same type of ion source (thermal desorption / electron impact ionisation), and consequently the observed organics fragmentation patterns were found to be comparable between the two instruments.

The capability of the IT-AMS to elucidate the structure of the fragmentation products observed in such mass spectra was demonstrated by an MS^4 study on tryptophan. Detection limits were found to be sufficiently low to allow for MS^2 studies on atmospheric particles under favourable ambient conditions (0.6 µg m^{-3} at a time resolution of 6 min in the given example), while MS$^{n>2}$ studies are only feasible at higher concentrations. Such a situation can be reached either under laboratory conditions, or via aerosol concentrator systems. All in all, we conclude that the IT-AMS can provide in-depth, quantitative information on total organic aerosol and on individual ion fragments both in field and in laboratory studies, and that these results are directly relatable to ToF-AMS results.

In laboratory studies on a variety of compounds, we found that the IT-AMS is capable of distinguishing $[C_4H_y]^+$ and $[C_3H_yO]^+$ fragments at the nominal m/z 55 and 57 via their characteristic fragmentation patterns in MS^2 experiments. Furthermore, it is possible to distinguish between fragments of the same elemental composition, but with different molecular structures: different characteristic MS^2 fragmentation patterns were found for the ions at m/z 60 and 73 for sugars and carboxylic acids, which have the same elemental compositions ($[C_2H_4O_2]^+$ / $[C_3H_5O_2]^+$) in both cases. While the fragment ions at these m/z originating from carboxylic acids and sugars therefore could not be differentiated with a ToF-AMS, the observed differences in their MS^2 fragmentation patterns could be used to distinguish between the two compound classes using the IT-AMS: MS^2 at m/z 60 yields average relative intensities of fragment ions m/z 43 to m/z 42 of 11 % / 100 % for carboxylic acids, but of 0 % / 100 % for sugars. Similarly, at m/z 73, the ratio of relative intensities of the MS^2 fragment ions m/z 45 to m/z 55 was on average 100 % / 3 % for sugars, but 32 % / 100 % for carboxylic acids.

More research is needed in order to further constrain these average values by testing a larger number of compounds, and by also testing substances from other compound classes for potential cross-sensitivities. However, these results already indicate that instruments like the IT-AMS potentially enable the distinction between carboxylic acids and sugars in organic aerosol by means of MS^2 experiments, which would further help on organic aerosol characterisation and source apportionment.

Acknowledgments

We thank Th. Böttger and the teams of the electronic and the mechanical workshops of the Max Planck Institute for Chemistry for their technical support and valuable help, especially M. Flanz, K.-H. Bückart, and M. Dieterich. We also thank J. Curtius and A. Kürten for their support and technical help regarding the initial design of the IT-AMS. P. Faber is gratefully acknowledged for providing some of the ToF-AMS data. Funding was provided by the Max Planck Institute for Chemistry and by the Institute for Atmospheric Physics at the Johannes Gutenberg University, Mainz.

References

Allan, J. D., Delia, A. E., Coe, H., Bower, K. N., Alfarra, M. R., Jimenez, J. L., Middlebrook, A. M., Drewnick, F., Onasch, T. B., Canagaratna, M. R., Jayne, J. T., and Worsnop, D. R.: A generalised method for the extraction of chemically resolved mass spectra from Aerodyne aerosol mass spectrometer data, J. Aerosol. Sci., 35, 909-922, 2004.

Canagaratna, M. R., Jayne, J. T., Jimenez, J. L., Allan, J. D., Alfarra, M. R., Zhang, Q., Onasch, T. B., Drewnick, F., Coe, H., Middlebrook, A., Delia, A., Williams, L. R., Trimborn, A. M., Northway, M. J., DeCarlo, P. F., Kolb, C. E., Davidovits, P., and Worsnop, D. R.: Chemical and microphysical characterization of ambient aerosols with the Aerodyne aerosol mass spectrometer, Mass Spectrometry Reviews, 26, 185- 222, 2007.

Cole, C. R., Outlaw, R. A., Champion, R. L., Baker, D. H., and Holloway, B. C.: Mass spectral resolution of F^+ and H_3O^+ in very high vacuum, Journal of Vacuum Science & Technology A, 21, 1796-1799, 2003.

DeCarlo, P. F., Kimmel, J. R., Trimborn, A., Northway, M. J., Jayne, J. T., Aiken, A. C., Gonin, M., Fuhrer, K., Horvath, T., Docherty, K. S., Worsnop, D. R., and Jimenez, J. L.: Field-Deployable, High-Resolution, Time-of-Flight Aerosol Mass Spectrometer, Analytical Chemistry, 78, 8281-8289, 2006.

Dotan, I., Hierl, P. M., Morris, R. A., and Viggiano, A. A.: Rate constants for the reactions of N^+ and N_2^+ with O_2 as a function of temperature (300–1800 K), International Journal of Mass Spectrometry and Ion Processes, 167, 223-230, 1997.

Drewnick, F., Hings, S. S., Alfarra, M. R., Prevot, A. S. H., and Borrmann, S.: Aerosol quantification with the Aerodyne Aerosol Mass Spectrometer: detection limits and ionizer background effects, Atmos. Meas. Tech., 2, 33-46, 2009.

Drewnick, F., Hings, S. S., DeCarlo, P., Jayne, J. T., Gonin, M., Fuhrer, K., Weimer, S., Jimenez, J. L., Demerjian, K. L., Borrmann, S., and Worsnop, D. R.: A New Time-of-Flight Aerosol Mass Spectrometer (TOF-AMS) - Instrument Description and First Field Deployment, Aerosol Science and Technology, 39, 637-658, 2005.

Fachinger, J. R. W.: Das Aerosol-Ionenfallen-Massenspektrometer (AIMS): Aufbau, Charakterisierung und Feldeinsatz, PhD thesis, Johannes Gutenberg University Mainz, Mainz, 2012.

Fuzzi, S., Baltensperger, U., Carslaw, K., Decesari, S., Denier van der Gon, H., Facchini, M. C., Fowler, D., Koren, I., Langford, B., Lohmann, U., Nemitz, E., Pandis, S., Riipinen, I., Rudich, Y., Schaap, M., Slowik, J. G., Spracklen, D. V., Vignati, E., Wild, M., Williams, M., and Gilardoni, S.: Particulate matter, air quality and climate: lessons learned and future needs, Atmos. Chem. Phys., 15, 8217-8299, 2015.

Goldstein, A. H. and Galbally, I. E.: Known and Unexplored Organic Constituents in the Earth's Atmosphere, Environ. Sci. Technol., 41, 1514-1521, 2007.

Hanna, S. J., Campuzano-Jost, P., Simpson, E. A., Robb, D. B., Burak, I., Blades, M. W., Hepburn, J. W., and Bertram, A. K.: A new broadly tunable (7.4–10.2 eV) laser based VUV light source and its first application to aerosol mass spectrometry, International Journal of Mass Spectrometry, 279, 134-146, 2009.

Harris, W. A., Reilly, P. T. A., and Whitten, W. B.: Detection of Chemical Warfare-Related Species on Complex Aerosol Particles Deposited on Surfaces Using an Ion Trap-Based Aerosol Mass Spectrometer, Analytical Chemistry, 79, 2354-2358, 2007.

Hierl, P. M., Dotan, I., Seeley, J. V., Van Doren, J. M., Morris, R. A., and Viggiano, A. A.: Rate constants for the reactions of O^+ with N_2 and O_2 as a function of temperature (300–1800 K), The Journal of Chemical Physics, 106, 3540-3544, 1997.

Hoffmann, T., Huang, R.-J., and Kalberer, M.: Atmospheric Analytical Chemistry, Analytical Chemistry, 83, 4649-4664, 2011.

Jayne, J. T., Leard, D. C., Zhang, X., Davidovits, P., Smith, K. A., Kolb, C. E., and Worsnop, D. R.: Development of an Aerosol Mass Spectrometer for Size and Composition Analysis of Submicron Particles, Aerosol Science and Technology, 33, 49-70, 2000.

Julian, R. K. and Cooks, R. G.: Broad-band excitation in the quadrupole ion trap mass spectrometer using shaped pulses created with the inverse Fourier transform, Analytical Chemistry, 65, 1827-1833, 1993.

Kanakidou, M., Seinfeld, J. H., Pandis, S. N., Barnes, I., Dentener, F. J., Facchini, M. C., Van Dingenen, R., Ervens, B., Nenes, A., Nielsen, C. J., Swietlicki, E., Putaud, J. P., Balkanski, Y., Fuzzi, S., Horth, J., Moortgat, G. K., Winterhalter, R., Myhre, C. E. L., Tsigaridis, K., Vignati, E., Stephanou, E. G., and Wilson, J.: Organic aerosol and global climate modelling: a review, Atmos. Chem. Phys., 5, 1053-1123, 2005.

Kürten, A., Curtius, J., Helleis, F., Lovejoy, E. R., and Borrmann, S.: Development and characterization of an ion trap mass spectrometer for the on-line chemical analysis of atmospheric aerosol particles, International Journal of Mass Spectrometry, 265, 30-39, 2007.

Kürten, C. A.: Entwicklung, Aufbau und Charakterisierung eines neuartigen Ionenfallen-Massenspektrometers für Aerosolpartikel (AIMS), PhD thesis, Johannes Gutenberg University Mainz, Mainz, 2007.

Liu, P., Ziemann, P. J., Kittelson, D. B., and McMurry, P. H.: Generating Particle Beams of Controlled Dimensions and Divergence: 1. Theory of Particle Motion in Aerodynamic Lenses and Nozzle Expansions, Aerosol Science and Technology, 22, 293-313, 1995.

March, R. E.: An introduction to quadrupole ion trap mass spectrometry, Journal of Mass Spectrometry, 32, 351-369, 1997.

McLafferty, F. W. and Tureček, F.: Interpretation of mass spectra, University Science Books, Sausalito, 1993.

Murphy, D. M.: The design of single particle laser mass spectrometers, Mass Spectrometry Reviews, 26, 150-165, 2007.

Ottens, A. K., Arkin, C. R., Griffin, T. P., Palmer, P. T., and Harrison, W. W.: Ion-molecule reactions in quadrupole ion trap mass spectrometry: implications for lightweight gas analysis, International Journal of Mass Spectrometry, 243, 31-39, 2005.

Pratt, K. A. and Prather, K. A.: Mass spectrometry of atmospheric aerosols—Recent developments and applications. Part I: Off-line mass spectrometry techniques, Mass Spectrometry Reviews, 31, 1-16, 2012.

Silva, P. J. and Prather, K. A.: Interpretation of mass spectra from organic compounds in aerosol time-of-flight mass spectrometry, Analytical Chemistry, 72, 3553-3562, 2000.

Sobanski, N., Tang, M. J., Thieser, J., Schuster, G., Pöhler, D., Fischer, H., Song, W., Sauvage, C., Williams, J., Fachinger, J., Berkes, F., Hoor, P., Platt, U., Lelieveld, J., and Crowley, J. N.: Chemical and meteorological influences on the lifetime of NO3 at a semi-rural mountain site during PARADE, Atmos. Chem. Phys., 16, 4867-4883, 2016.

SQUIRREL: http://cires.colorado.edu/jimenez-group/ToFAMSResources/ToFSoftware/index.html, last access: 14.07.2016, 2016.

Sun, Y.-L., Zhang, Q., Schwab, J. J., Demerjian, K. L., Chen, W.-N., Bae, M.-S., Hung, H.-M., Hogrefe, O., Frank, B., Rattigan, O. V., and Lin, Y.-C.: Characterization of the sources and processes of organic and inorganic aerosols in New York city with a high-resolution time-of-flight aerosol mass apectrometer, Atmos. Chem. Phys., 11, 1581-1602, 2011.

Thornberry, T., Murphy, D. M., Thomson, D. S., de Gouw, J., Warneke, C., Bates, T. S., Quinn, P. K., and Coffman, D.: Measurement of Aerosol Organic Compounds Using a Novel Collection/Thermal-Desorption PTR-ITMS Instrument, Aerosol Science and Technology, 43, 486-501, 2009.

Vogel, A. L., Äijälä, M., Brüggemann, M., Ehn, M., Junninen, H., Petäjä, T., Worsnop, D. R., Kulmala, M., Williams, J., and Hoffmann, T.: Online atmospheric pressure chemical ionization ion trap mass spectrometry (APCI-IT-MS[n]) for measuring organic acids in concentrated bulk aerosol - a laboratory and field study, Atmos. Meas. Tech., 6, 431-443, 2013.

Wu, H.-F. and Brodbelt, J. S.: Effects of collisional cooling on ion detection in a quadrupole ion trap mass spectrometer, International Journal of Mass Spectrometry and Ion Processes, 115, 67-81, 1992.

Zhang, Q., Jimenez, J. L., Canagaratna, M. R., Ulbrich, I. M., Ng, N. L., Worsnop, D. R., and Sun, Y.: Understanding atmospheric organic aerosols via factor analysis of aerosol mass spectrometry: a review, Analytical and Bioanalytical Chemistry, 401, 3045-3067, 2011.

Table 1: Organic substances investigated in the laboratory studies. All purities were ≥98 %.

Compound	Structural formula	Molecular formula	Molecular weight / g mol^{-1}
Butyl valerate		$C_9H_{18}O_2$	158.24
Glucose		$C_6H_{12}O_6$	180.16
Glutaric acid		$C_5H_8O_4$	132.12
Glutathione		$C_{10}H_{17}N_3O_6S$	307.32
Levoglucosan		$C_6H_{10}O_5$	162.14
Mannitol		$C_6H_{14}O_6$	182.17
Oleic acid		$C_{18}H_{34}O_2$	282.47
PEG200 [a]		$C_{2n}H_{4n+2}O_{n+1}$	~200 [b]
cis-Pinonic acid		$C_{10}H_{16}O_3$	184.23
Saccharose		$C_{12}H_{22}O_{11}$	342.30
Succinic acid		$C_4H_6O_4$	118.09
Tryptophan		$C_{11}H_{12}N_2O_2$	204.23
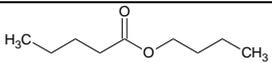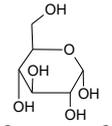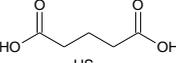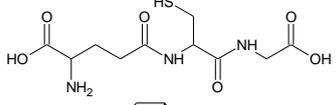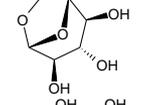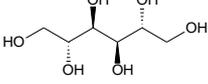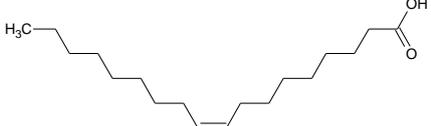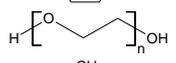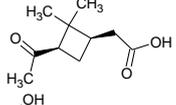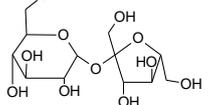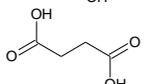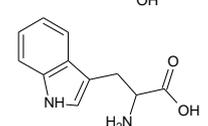
[a] Polyethylene glycol. [b] Average molecular mass.

Table 2: IT-AMS operating parameters in the MS^n studies. V_{RF} is the amplitude (zero-to-peak) of the radiofrequency drive voltage (1.3 MHz) applied to the ring electrode; q_z is the stability parameter resulting from the Mathieu equation (March, 1997). The resonance frequency was experimentally determined.

| | Trapping phase | | | Reaction phase | | | Resonant excitation | |
| | | | | | | | | |
m/z	Duration / ms	V_{RF} / V	q_z	Duration / ms	V_{RF} / V	q_z	Amplitude / mV	Frequency / kHz
130	50	700	0.303	150	700	0.303	80	118.5
103	50	700	0.383	150	700	0.383	80	150
77	50	700	0.512	100	700	0.512	120	202
73	50	258 – 287	0.206 – 0.228	100	402	0.320	120	152.5
60	50	258 – 287	0.25 – 0.278	100	402	0.389	120	186.5
57	50	258 – 287	0.263 – 0.296	100	402	0.409	120	196.5
55	50	258 – 287	0.273 – 0.314	100	402	0.424	120	204.5
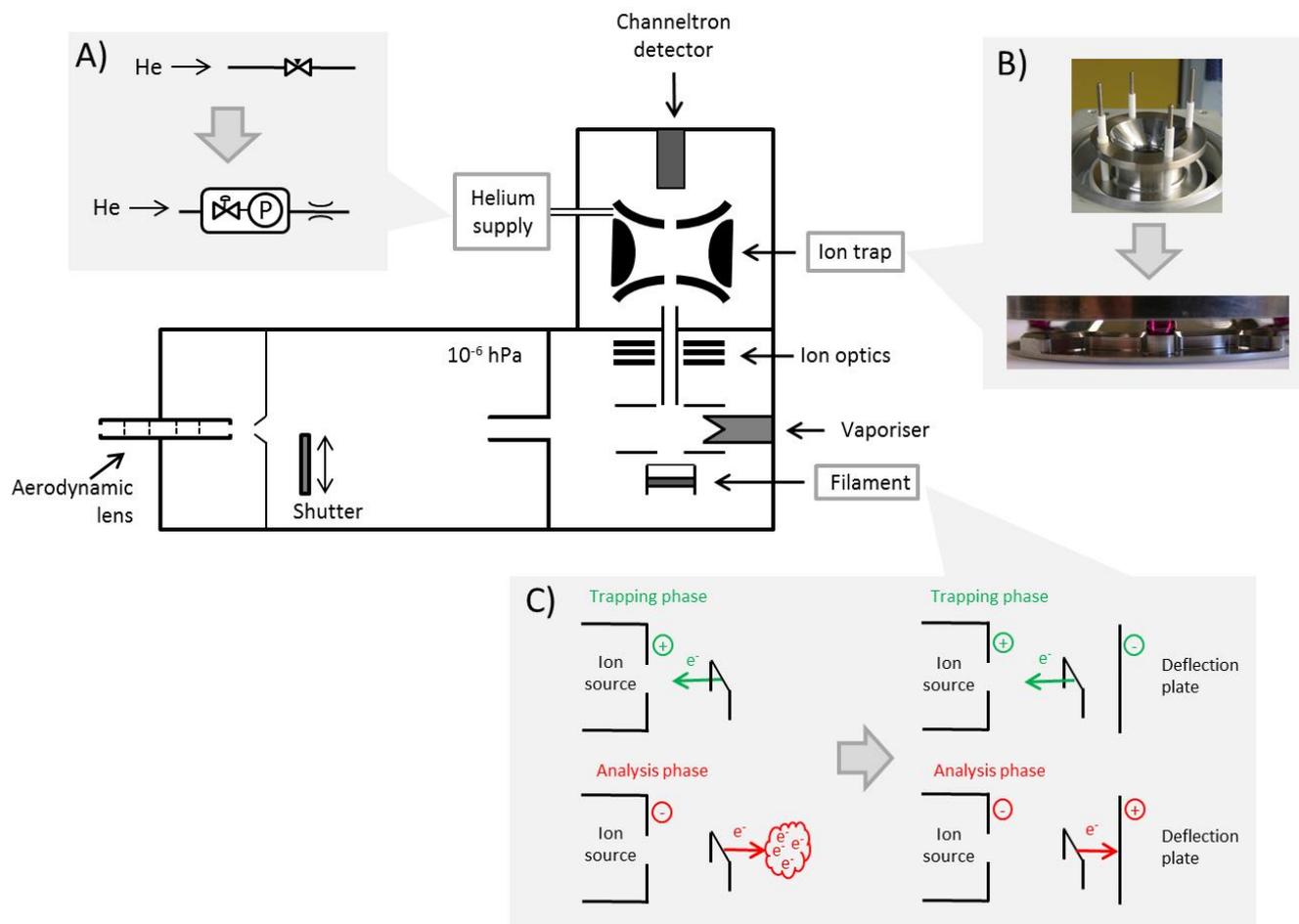
Figure 1: Schematics of the IT-AMS. The insets A-C visualise the major hardware modifications (compared to Kürten et al., 2007) described in the main text.
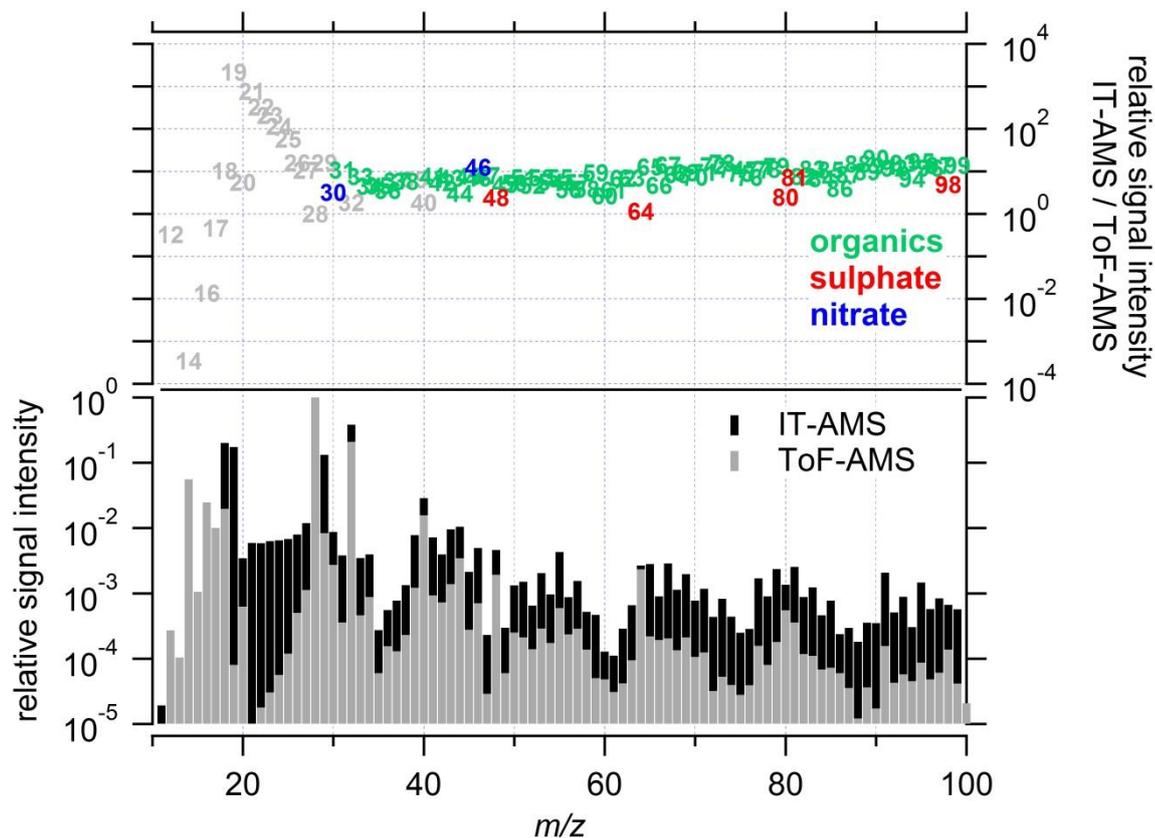
Figure 2: Comparison of average mass spectra measured with the IT-AMS and the ToF-AMS during 11-day long ambient measurements. Shown are the average mass spectra normalised to *m/z* 28 (bottom panel) and the ratio (IT-AMS to ToF-AMS) of these relative signal intensities, colour-coded for the dominant species at the respective *m/z* (upper panel).
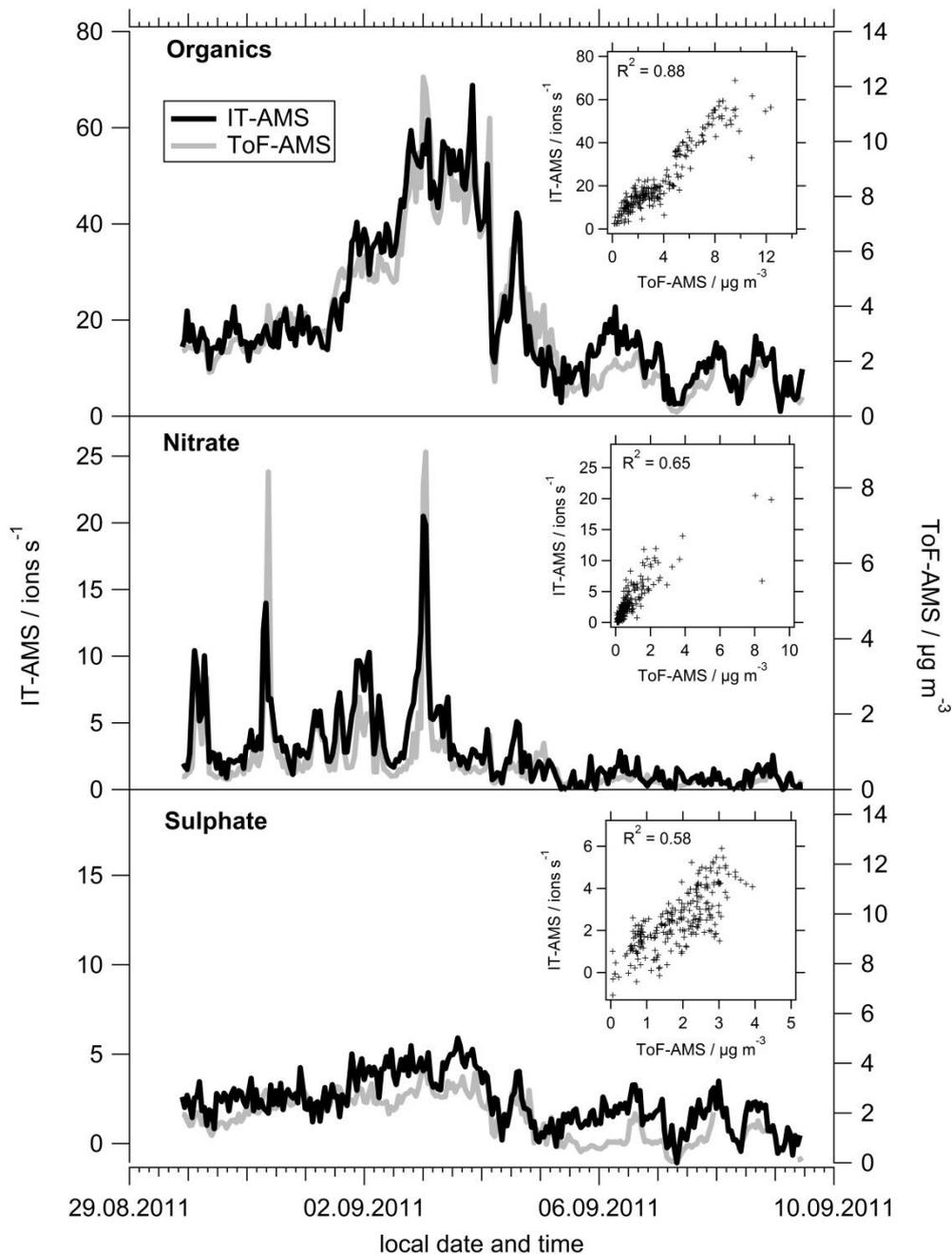
Figure 3: Comparison of 1 h-averaged time series of organics (upper panel), nitrate (middle panel) and sulphate (lower panel) measured with the IT-AMS (left axis) and the ToF-AMS (right axis) during 11-day long ambient measurements. The inlays show the correlation of the respective time series and the associated squared Pearson's correlation coefficient (R^2).
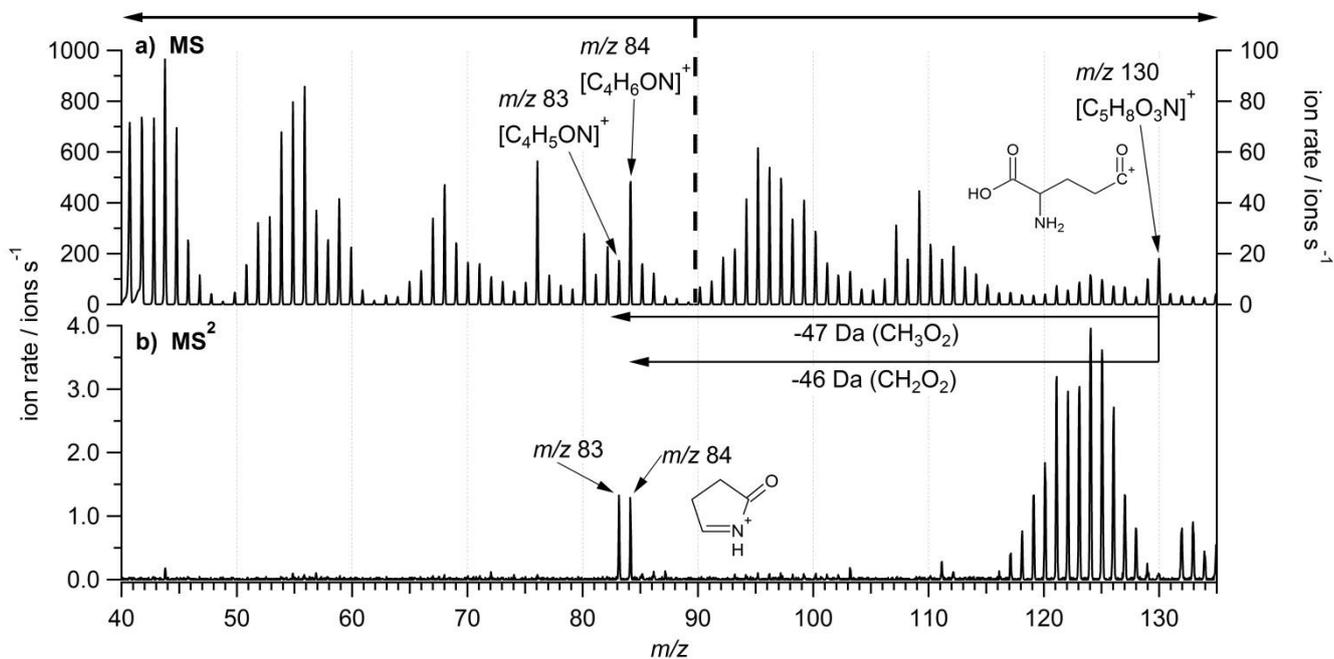
Figure 4: MS² study on glutathione. Shown are the "classic" MS (a) and the mass spectrum acquired after isolating and fragmenting *m/z* 130 (MS², b). The signal in b) in the *m/z* range ~120 – 130 originates from ions remaining after the isolation step.
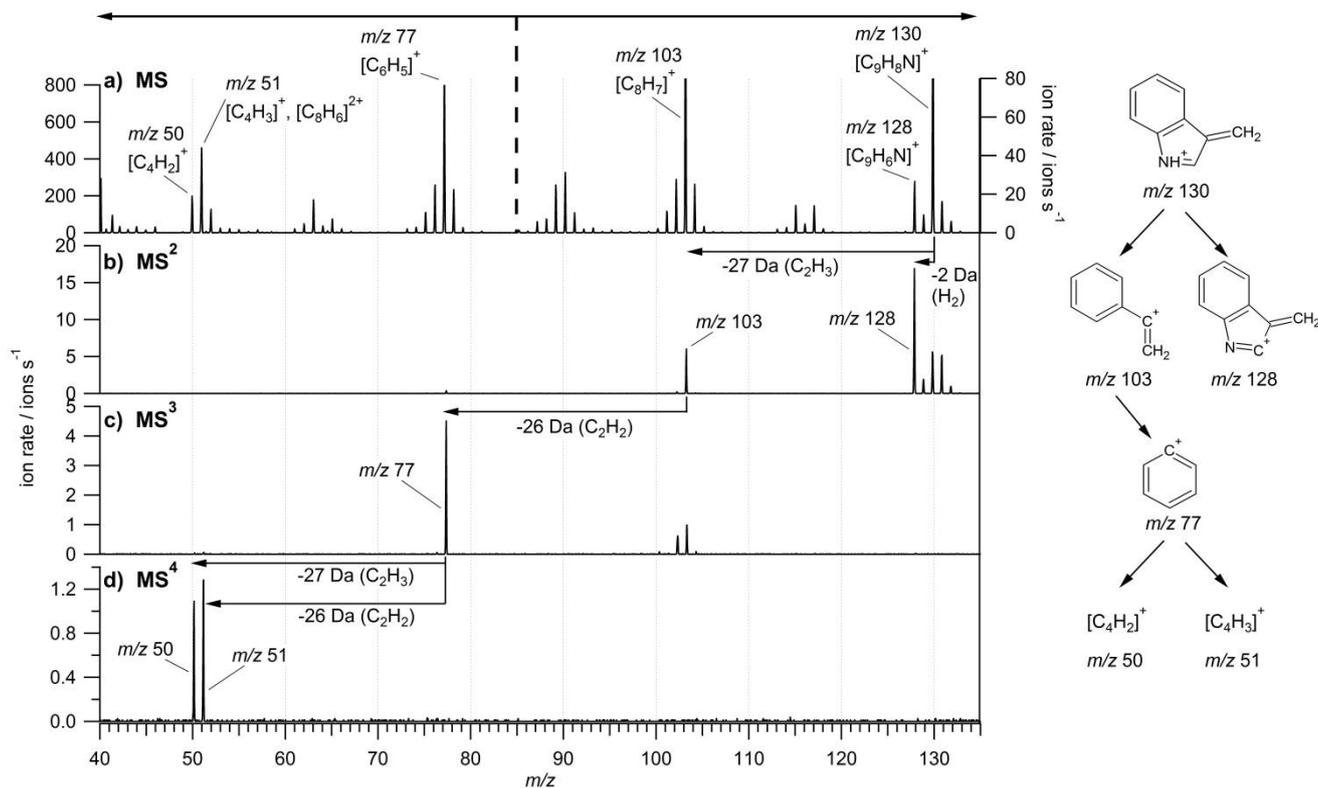
Figure 5: MS^4 study on tryptophan. Shown are the "classic" MS (a) and mass spectra acquired after isolating and fragmenting *m/z* 130 (MS^2, b), *m/z* 103 (MS^3, c), and *m/z* 77 (MS^4, d) from the respective previous step.
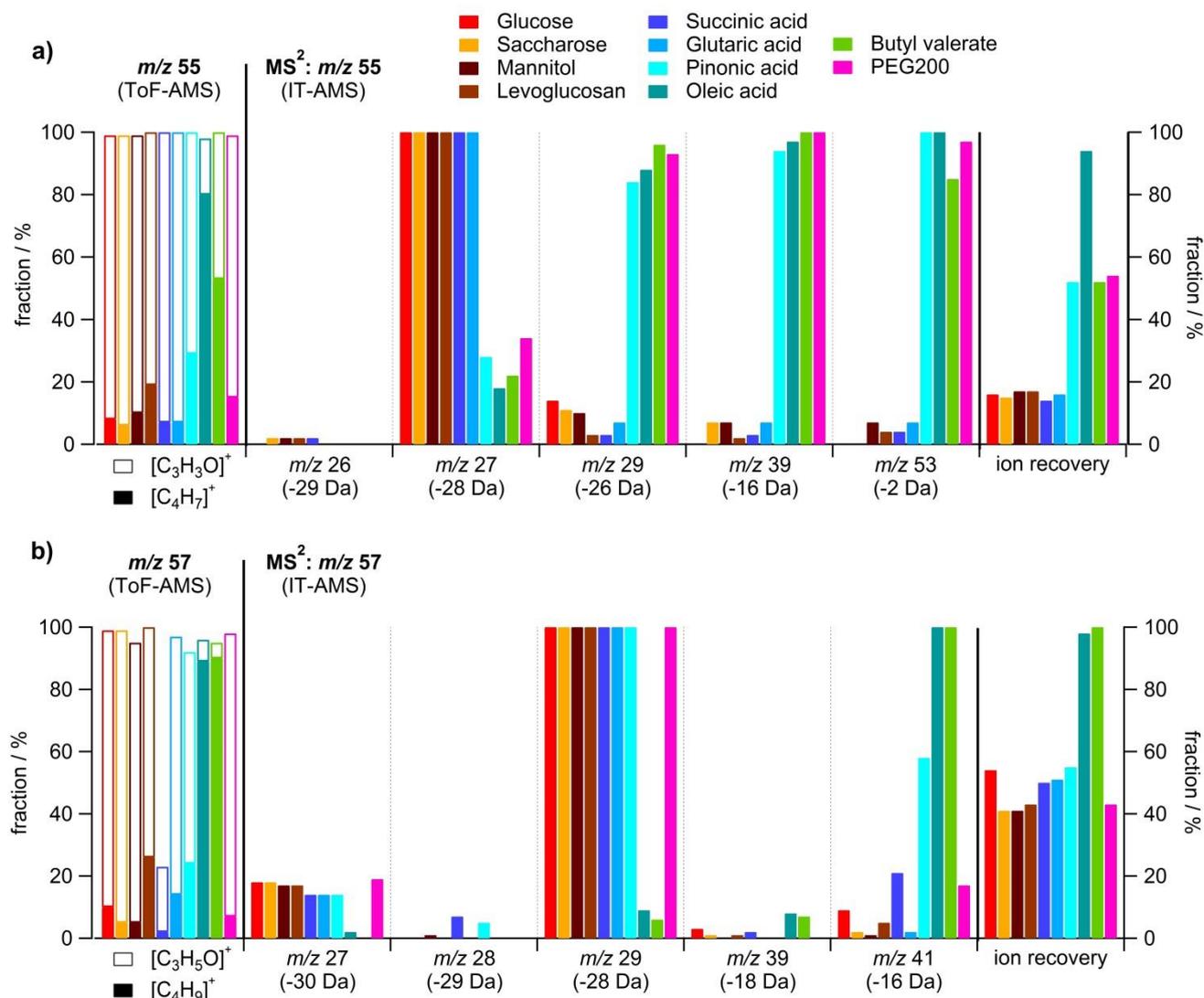
Figure 6: Results of studies on (a) *m/z* 55 and (b) *m/z* 57 for various compounds. On the left, the relative contributions of [C_3H_3O]$^+$ and [C_4H_7]$^+$ to *m/z* 55 and of [C_3H_5O]$^+$ and [C_4H_9]$^+$ to *m/z* 57 are given (from ToF-AMS measurements). On the right, the results from IT-AMS MS^2 studies on these ions are summarised. For each investigated compound, the signal intensity of the fragment ions (relative to the signal intensity of the most abundant fragment) and the ion recovery are given. Not shown are fragments accounting for less than 1 % and, for the MS^2 experiment on *m/z* 57, small contributions observed at fragment ion *m/z* 31 for mannitol (1 % relative fraction) and at *m/z* 42 for glucose, oleic acid, and butyl valerate (3 %, 1 %, and 3 % relative fraction).
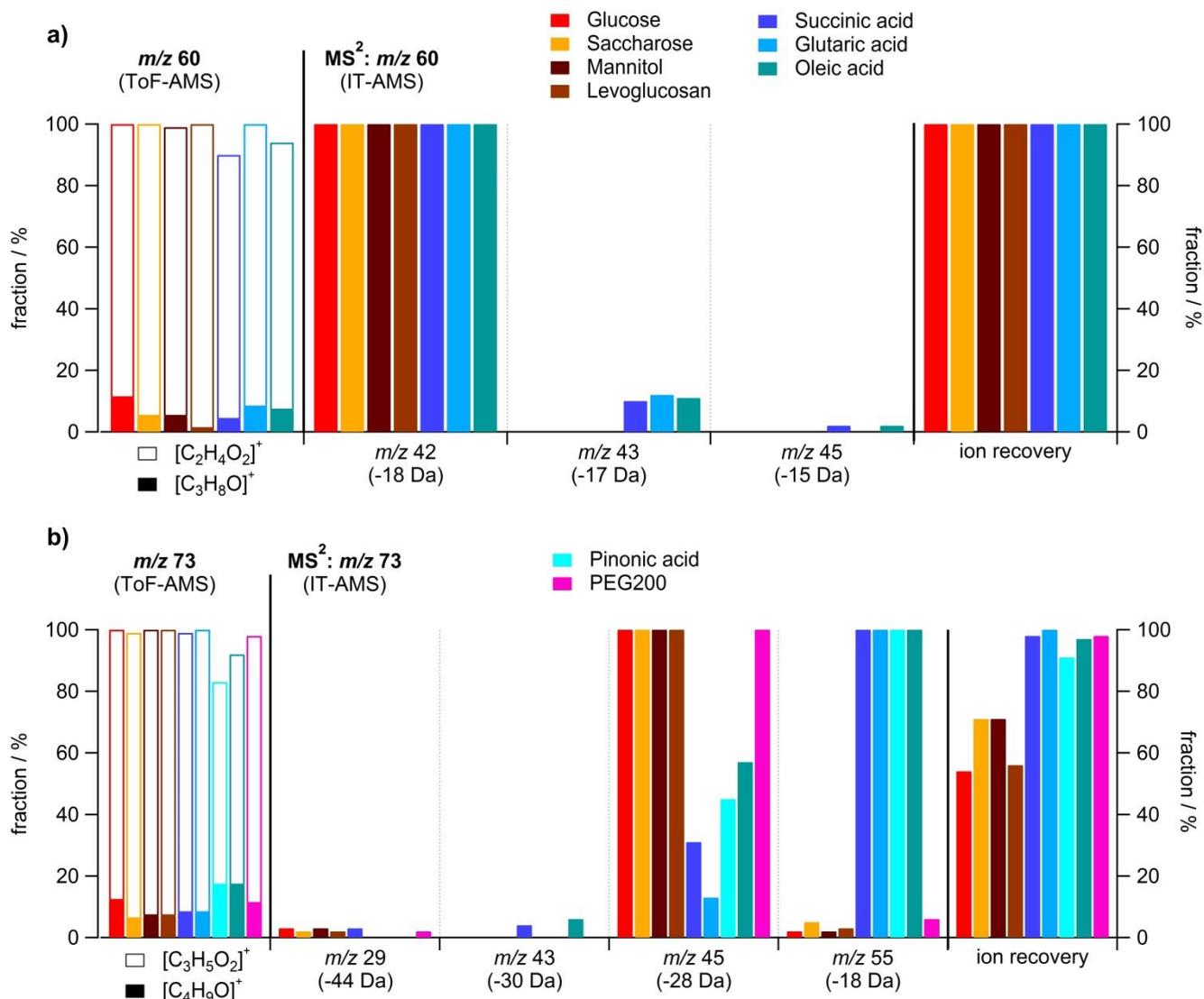
Figure 7: Results of studies on (a) *m/z* 60 and (b) *m/z* 73 for various compounds. On the left, the relative contributions of $[C_2H_4O_2]^+$ and $[C_3H_8O]^+$ to *m/z* 60 and of $[C_3H_5O_2]^+$ and $[C_4H_9O]^+$ to *m/z* 73 are given (from ToF-AMS measurements). On the right, the results from IT-AMS MS^2 studies on these ions are summarised. For each investigated compound, the signal intensity of the
5 **fragment ions (relative to the signal intensity of the most abundant fragment) and the ion recovery are given. Not shown are fragments accounting for less than 1 % and, for the MS^2 experiment on *m/z* 73, a small contribution observed at fragment ion *m/z* 61 for glucose (2 % relative fraction).**